Pelras, Théophile; Mahon, Clare S.; Nonappa, Nonappa; Ikkala, Olli; Gröschel, André H.; Müllner, Markus

Polymer Nanowires with Highly Precise Internal Morphology and Topography

Polymer Nanowires with Highly Precise Internal Morphology and Topography

Théophile Pelras,[†,‡] Clare S. Mahon,[†,¶] Nonappa,[§] Olli Ikkala,[§] André H. Gröschel,[‖] and Markus Müllner*[†,‡]

[†]School of Chemistry, Key Centre for Polymers and Colloids, The University of Sydney, Sydney, 2006 New South Wales, Australia

[‡]The University of Sydney Nano Institute, Sydney, 2006 New South Wales, Australia

[§]Department of Applied Physics, Aalto University School of Science, Puumiehenkuja 2, FIN-02150 Espoo, Finland

[‖]Physical Chemistry and Center for Nanointegration Duisburg-Essen (CENIDE), University of Duisburg-Essen, 47057 Duisburg, Germany

S *Supporting Information*

ABSTRACT: The construction of precise soft matter nanostructures in solution presents a challenge. A key focus remains on the rational design of functionalities to achieve the high morphological complexity typically found in biological systems. Advances in controlled polymerizations and self-assembly increasingly allow approaches toward complex hierarchical nanomaterials. By combining tailor-made cylindrical polymer brushes, block copolymers and interpolyelectrolyte complexation-driven self-assembly, we demonstrate a facile construction of uniformly compartmentalized and topographically structured polymeric nanowires in aqueous media. The approach offers a modular avenue in programming the internal morphology of polymer nanowires by varying the block copolymer composition and topology.

Many systems in nature reveal a superior ability to compartmentalize functionality and arrange chemistries in three dimensions. Similarly, precise solution-based synthetic soft-matter nanostructures are being pursued; however, their build-up is challenging as it requires a detailed control of the structure formation and the underlying processes.[1−3] While DNA nanotechnology already allows rationally engineered nanostructures with high precision,[4,5] multiblock polymers, particularly diblock copolymers (DBs), still lack comparable structuring capabilities despite their widespread use in many applications. Taken that the underlying design principles for complex structures are mastered for DBs, they could offer robust and cost-effective alternatives.[6] Their self-assembly is driven by relatively weak competing interactions between the polymer blocks and the solvent, additionally allowing control via external stimuli (e.g., solvent changes, pH, temperature)[7] or by incorporating supramolecular interactions.[8] The immense potential of block copolymers for the construction of complex solvent-based nanostructures has been demonstrated by their assembly to multicompartment nanoparticles and their subsequent assembly to higher orders.[2,8,9] A different approach uses crystallization-driven self-assembly of DBs from seed particles to produce dispersions of complex, compartmentalized 1D and 2D assemblies.[3,10] A simple, yet powerful, method

for hierarchical supramolecular polymer self-assembly builds on the electrostatic complexation between polyanions and polycations,[11] where interpolyelectrolyte complexation (IPEC) enables the formation of nanostructured and multicompartment polymer particles in solution. While IPECs were originally used to produce micelles,[12−16] vesicles,[17,18] or multilayered architectures,[19−22] they have recently exemplified their potential as a powerful tool to interact with polymer particles, leading to polymer architectures that are otherwise difficult to realize.[23] For example, homopolymer complexation onto polymer micelles has yielded multicompartment particles with collapsed and patchy shells.[24] Patchy morphology can also be induced via intramolecular complexation on a core−shell cylinder carrying both positive and negative charges in its shell.[25] Using DBs containing a neutral and charged block, oppositely charged micelles can be switched charge-neutral, and subsequently used in photodynamic therapy.[26] Recently, IPECs have also shown potential in the design of non-equilibrium polymer micelles capable of reversibly switching their assembly upon change of temperature or salt concentration.[16] Elegant structures via complexation of DBs onto soft templates have been predicted—ranging from spherical micelles to fibrillar (1D) and discoidal/planar (2D) particulates.[27]

An intriguing 1D polymer nanomaterial (i.e., template material) are cylindrical polymer brushes (CPBs) (also known as molecular brushes, bottlebrush polymers, or comb-shaped polymers) allowing a high level of control over backbone and side chain lengths, and their distribution.[28] CPBs are densely grafted polymers which can avoid chain entanglement and exist as unimolecular entities. Given their covalent construction and unique architecture, they find increasing use in self-assembly,[29] nanomedicine[30] or as polymer scaffolds to produce tailor-made organic and inorganic (nano)materials.[31−36]

In this work, we designed core−shell polyelectrolyte CPBs as 1D templates and used IPECs to produce centipede-like polymer nanowires with uniform topographical features and internal compartmentalization along the CPB backbone (Scheme 1).

Scheme 1. Design Process To Produce IPEC-structured, Centipede-like Polymer Nanowires[a]
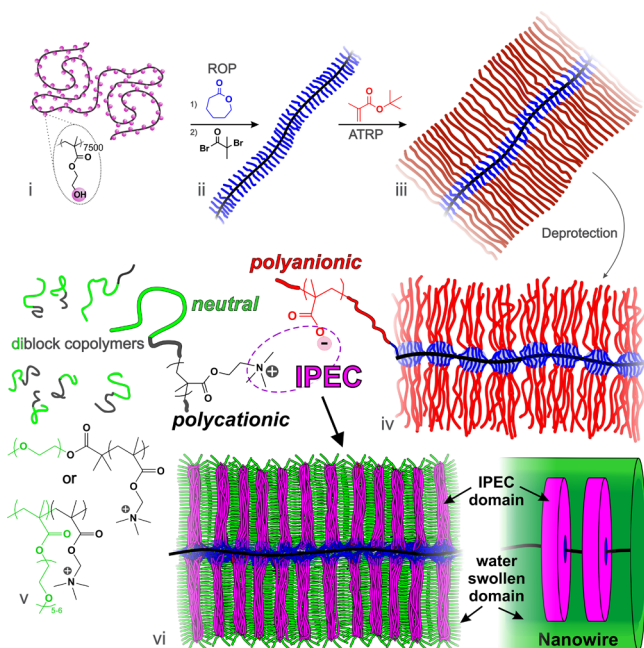
[a](i) PHEMA is sequentially grafted-from with ε-caprolactone (ii) and tBMA to yield (iii) core−shell CPBs that after deprotection form (iv) 1D polyelectrolyte templates with a pearl-necklace core structure. IPEC formation with (v) oppositely charged DBs yields (vi) uniformly structured nanowires featuring IPEC discs along the long-axis.

The template was synthesized by first grafting polycaprolactone (PCL) from a high-molecular weight poly-(hydroxyethyl methacrylate) (PHEMA$_{7500}$) backbone via ring-opening polymerization. The terminal hydroxy groups of the PHEMA$_{7500}$-g-PCL$_{14}$ homopolymer side chains were modified with α-bromoisobutyrate initiators,[33] to allow the grafting of a poly(tert-butyl methacrylate) (PtBMA) shell using atom transfer radical polymerization (ATRP) (Scheme 1, Figure S1). Monomer conversion was monitored by proton nuclear magnetic resonance (^{1}H NMR) spectroscopy, which was used to calculate the side chain length, based on reported grafting efficiencies from PHEMA polyinitiator backbones[37] and PCL CPBs[33] (Figure S2).

Removal of the tert-butyl groups with trifluoroacetic acid, followed by dispersion in an alkaline buffer solution (pH 10) yielded negatively charged polyelectrolyte polycaprolactone-block-poly(methacrylic acid) core−shell CPBs, namely PHEMA$_{7500}$-g-[PCL$_{14}$-b-PMAA$_{300}$]. The complete removal of the tert-butyl groups was confirmed by the disappearance of the characteristic signal at 1.4 ppm in the ^{1}H NMR spectrum of the CPB (Figure S3-1), combined with Fourier-transform infrared spectroscopic (FTIR) analysis (Figure S3-2).

The worm-like conformation of the core−shell brushes was studied by atomic force microscopy (AFM). Before deprotection, the hydrophobic CPB templates formed "monolayer islands" on mica upon solvent evaporation (THF), with core and shell clearly visible (Figure S4-1). After deprotection, the morphology of the polyelectrolyte template brushes in aqueous solution revealed individual cylindrical brush particles (Figure 1A, Figure S4-2). AFM height analysis indicated significant roughness due to CPB core segmentation. AFM analysis in the
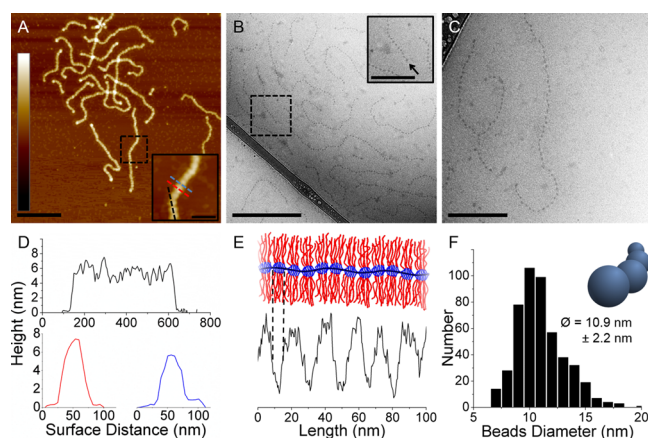

Figure 1. AFM height image of CPBs drop-cast from pH 10 buffer onto mica (A). Cryo-TEM images in pH 10 buffer (B, C). AFM cross-sectional analysis across several beads (black), across a single bead (red) and between two beads (blue) (D). Gray-scale analysis across the beads (arrow in panel B) (E). Statistical analysis of bead diameters (data extracted from 500 beads in several images) (F). Scale bars: (A, B) 500 nm, (B inset, C) 200 nm, (A inset) 100 nm. AFM z-scale: ± 20 nm.

dry state (Figure 1D) revealed cross-sectional heights from 5 nm (between two beads, blue plot) to 8 nm (on top of beads, red plot), with apparent flattening due to solvent evaporation. Cryogenic transmission electron microscopy (cryo-TEM) better highlighted the distinct pearl-necklace structure, where the hydrophobic PCL core minimizes its interaction with water to form spherical "pearls" or "beads" along the brush backbone (Figures 1B,C and Figure S5), suggesting a distinct core compartmentalization along the brush long-axis. A gray scale analysis revealed a constant bead-to-bead distances (8.1 ± 2.6 nm, Figure 1E) and a narrow distribution of the bead diameters (10.9 ± 2.2 nm, Figure 1F).

Next, we synthesized bis-hydrophilic DBs containing a poly(2-dimethylamino ethyl methacrylate) (PDMAEMA) block as well as either a linear poly(ethylene oxide) (PEO) or comb-like poly(ethylene glycol) methyl ether methacrylate (PEGMA) blocks (Figure S1). The DB syntheses are described in the Supporting Information (Figures S6 and S7, and Table S2). PDMAEMA was quaternized with methyl iodide following a published procedure[33] to yield copolymers with a positively charged poly[2-(methacryloyloxy)ethyl trimethylammonium iodide] (PMETAI) block and a nonionic (PEO or PEGMA) block. The quaternization enabled IPEC formation at alkaline pH, at which PDMAEMA would otherwise be water-insoluble.

We next explored the formation of IPECs between the polyelectrolyte brush and oppositely charged DBs. The IPEC-structured polymer nanowires are denoted as nanowire-X (X represents the DB used for the formation). To produce the nanowires, the CPB template and DBs were mixed in alkaline suspensions using nominally stoichiometric ratios of the negative and positive charges to compensate all charges. For nanowire-A, formed by complexing PEO$_{114}$-b-PMETAI$_{45}$ (DB-A) onto the CPB, 6−7 chains of DB-A vs one PMAA$_{300}$ brush side chain were required to achieve charge neutrality. After IPEC formation, AFM revealed a significant surface roughness along the nanowire. While the cross-sectional height showed only a slight increase of ca. 25% (Figure S8-1), the nanowires showed a more pronounced pearl-necklace structure in the dry

state upon deposition onto mica (Figure S8-2) compared to the pristine brush template.

Cryo-TEM revealed remarkably regular patterns along the backbone (Figure 2). This suggested directed DB self-assembly
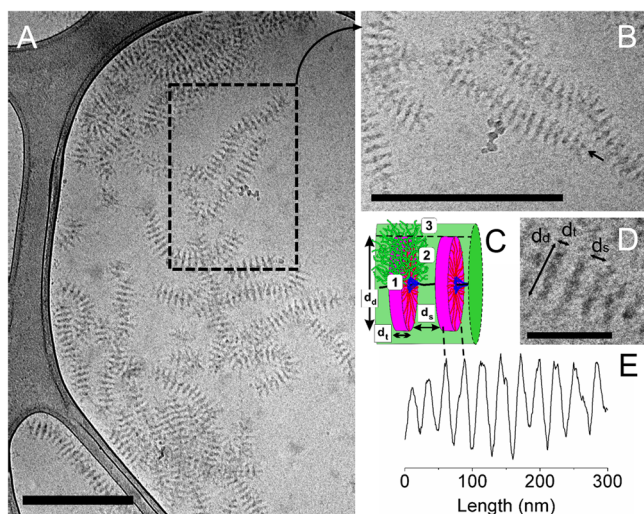

Figure 2. Cryo-TEM image of nanowire-A displaying centipede-like architectures in pH 10 buffer (A, B). Scheme illustrating various features within a nanowire (C) and an exemplary micrograph (D) and gray scale analysis (E) of one nanowire extracted from (B). Scale bars: (A, B) 500 nm, (D) 100 nm.

along the CPB templates with the hydrophobic IPEC domains (i.e., PMAA/PMETAI-domains, complexed by stoichiometric charges of the polyanion and polycation[6] indicated as 1 in Figure 2C) and hydrophilic PEO domains (indicated as 2 in Figure 2C) leading to their mutual repulsion. IPECs showed enhanced contrast in TEM, while PEO between or beyond the IPEC (Figure 2D; regions 2 and 3 in Figure 2C) was highly swollen with water and therefore not resolved. The IPEC appeared to be a lamellar disc, with disc diameter ($d_{d\ IPEC-A}$) of 59.3 ± 9.2 nm, stacked between PEO domains and perpendicular to the backbone of the template brushes. Each disc within nanowire-A was separated by regular distances (disc-to-disc spacing, $d_{s\ IPEC-A} = 14.0 \pm 2.7$ nm), which is dictated by the stabilizing PEO block that is sandwiched between the IPEC discs (Figure 1C). Similarly, the average disc thickness ($d_{t\ IPEC-A}$) of 11.0 ± 1.8 nm was very uniform (Table 1). A trade-off between minimizing the IPEC/water interface and generating sufficient space for the PEO chains ultimately drives the formation of this morphology. The volumes occupied by the IPEC (~44 vol%) and the water-swollen PEO (~56 vol%) confined within the nanowire, also suggested a lamellar arrangement of the hydrophobic and hydrophilic domains.

To investigate the effect of the DB composition, we next used PMETAI$_{48}$-b-PEGMA$_{103}$ (DB-B) for the complexation. DB-B had a similar number of repeat units to DB-A, but due to the different molecular weights of the repeat units of the nonionic blocks (PEGMA = 300 g·mol^{-1} vs PEO = 44 g·mol^{-1}), the fraction of the nonionic block was much higher. The similar PMETAI block length meant however that 6−7 copolymer chains per brush side chain were still needed to compensate the charges during nanowire-B formation. Thus, we could directly compare the effect of a larger nonionic block fraction on the IPEC formation and resulting nanowire morphology. In comparison to nanowire-A, this resulted in a less organized assembly, with less well-defined internal IPEC structures. The bulkiness of PEGMA led to more chain crowding and the increasing volume demand could not accommodate the formation of regular discs but forced the IPEC domains to develop distinct protrusions (Figure 3D−F). The higher steric demand was further reflected in the increased feature spacing ($d_{s\ IPEC-B} = 22.9 \pm 5.4$ nm).
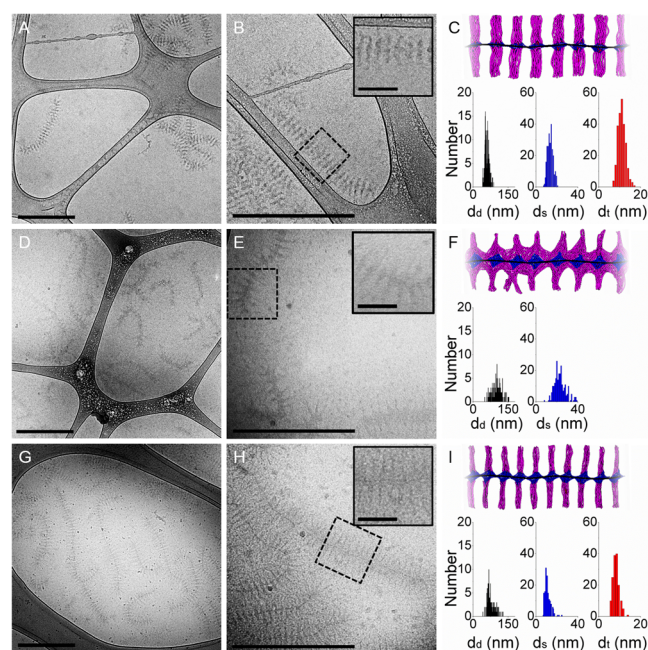

Figure 3. Cryo-TEM images, schematic cross sections and statistical analyses of disc diameter, thickness, and spacing of nanowire-A (A−C), nanowire-B (D−F) and nanowire-C (G−I). Scale bars: (A−H) 500 nm, (insets) 100 nm. Data extracted from various cryo-TEM images on >150 discs.

Finally, we used PMETAI$_{25}$-b-PEGMA$_{76}$ (DB-C) to form nanowire-C. The block ratio was comparable to DB-B, but due to the relatively shorter PMETAI block, double the number of polymer chains (~12) of DB-C are needed for charge

Table 1. Overview of DB Composition and IPEC-Induced Nanowire Features

Composition	charged/uncharged weight ratio	M_n (kDa)	nanowire	Disc diameter, d_d (nm)	Disc-to-disc spacing, d_s (nm)	Disc thickness, d_t (nm)
PMETAI$_{45}$-b-PEO$_{114}$ (DB-A)	73/27	18	A	59.3 ± 9.2	14.0 ± 2.7	11.0 ± 1.8
PMETAI$_{48}$-b-PEGMA$_{103}$ (DB-B)	32/68	45	B	100.7 ± 20.7	22.9 ± 5.4	
PMETAI$_{25}$-b-PEGMA$_{76}$ (DB-C)	25/75	30	C	76.7 ± 16.3	11.6 ± 2.9	8.6 ± 1.5

^{a}Determined via ^{1}HNMR. ^{b}Determined via gray scale analysis of cryo-TEM images (as indicated in Figure 2).

compensation. The reduced molecular weight allowed nanowire-C to again develop a lamellar IPEC pattern (Figure 3G–I), albeit thinner ($d_{t\ IPEC-C} = 8.6 \pm 1.5$ nm) than in nanowire-A due to the shorter PMETAI block length. Comparable occupied volumes (~43 vol % IPEC, ~57 vol % PEGMA) yielded IPEC discs featuring uniform diameters ($d_{d\ IPEC-C} = 76.7 \pm 16.3$ nm) and disc-to-disc spacings ($d_{s\ IPEC-C} = 11.6 \pm 2.9$ nm). Considering the regularity of the bead distance (center-to-center, 19.0 ± 2.5 nm) in the template brush, the center-to-center distance between each disc (Table S4) matched that of nanowire-A (25.0 ± 4.5 nm) and nanowire-C (20.2 ± 4.4 nm). We propose that the preorientation of the side chains in the pearl-necklace structure of the template brush directs the regular distances of the forming IPEC structures. The formation of lamellar discs is likely to result from our flexible brush template, as a previous study on stiff cellulose nanocrystals has shown IPECs would energetically favor the formation of IPEC helices along the long axis.[38]

In conclusion, nanostructured 1D soft matter can be accessed from a stoichiometric complexation of core–shell polyelectrolyte brush templates and bis-hydrophilic DBs containing a neutral- and oppositely charged block. A regular disc-like lamellar self-assembly directed along the cylindrical polymer brush axis was observed (Figures S9 and S10, and videos). The well-defined and uniform patterns, i.e., compartments along the 1D polymer backbone, can be tailored by varying DB molecular weight, composition and topology. Altering the number of complexing polymer chains can be a means to alter the overall structure and disc thickness, while changing the DB molecular weight and block ratio showed a significant effect on nanowire morphology and developed features. Combining the highly modular brush synthesis and the tunable structuring approach using IPEC formation may open further avenues toward nanoarchitectures featuring increasing complexity and topographical features, and lead to opportunities to arrange surface chemistries in ways that mimic bioactive nanoparticles (e.g., viruses) or brush-on-brush structures (e.g., proteoglycan aggregates).

ASSOCIATED CONTENT

Ⓢ Supporting Information

The Supporting Information is available free of charge on the ACS Publications website at DOI: 10.1021/jacs.8b08870.

> 3D reconstruction video of Nanowire C (multiple nanowires) (AVI)
>
> 3D reconstruction video of Nanowire C (one nanowire) (AVI)
>
> Materials, methods, experimental details, and additional characterization data (NMR, IR, SEC, AFM, cryo-EM) (PDF)

AUTHOR INFORMATION

Corresponding Author

*markus.muellner@sydney.edu.au

ORCID Ⓞ

Nonappa: 0000-0002-6804-4128
Olli Ikkala: 0000-0002-0470-1889
André H. Gröschel: 0000-0002-2576-394X
Markus Müllner: 0000-0002-0298-554X

Present Address

¶Department of Chemistry, University of York, Heslington, York YO10 5DD, U.K.

Notes

The authors declare no competing financial interest.

REFERENCES

(1) Chen, Q.; Bae, S. C.; Granick, S. Directed self-assembly of a colloidal kagome lattice. *Nature* **2011**, *469*, 381−384.

(2) Gröschel, A. H.; Schacher, F. H.; Schmalz, H.; Borisov, O. V.; Zhulina, E. B.; Walther, A.; Müller, A. H. E. Precise hierarchical self-assembly of multicompartment micelles. *Nat. Commun.* **2012**, *3*, 710.

(3) Li, X.; Gao, Y.; Boott, C. E.; Winnik, M. A.; Manners, I. Non-covalent synthesis of supermicelles with complex architectures using spatially confined hydrogen-bonding interactions. *Nat. Commun.* **2015**, *6*, 8127.

(4) He, Y.; Ye, T.; Su, M.; Zhang, C.; Ribbe, A. E.; Jiang, W.; Mao, C. Hierarchical self-assembly of DNA into symmetric supramolecular polyhedra. *Nature* **2008**, *452*, 198−201.

(5) Douglas, S. M.; Dietz, H.; Liedl, T.; Högberg, B.; Graf, F.; Shih, W. M. Self-assembly of DNA into nanoscale three-dimensional shapes. *Nature* **2009**, *459*, 414−418.

(6) Schacher, F. H.; Rupar, P. A.; Manners, I. Functional Block Copolymers: Nanostructured Materials with Emerging Applications. *Angew. Chem., Int. Ed.* **2012**, *51* (32), 7898−7921.

(7) Tritschler, U.; Pearce, S.; Gwyther, J.; Whittell, G. R.; Manners, I. 50th Anniversary Perspective: Functional Nanoparticles from the Solution Self-Assembly of Block Copolymers. *Macromolecules* **2017**, *50* (9), 3439−3463.

(8) Cui, H.; Chen, Z.; Zhong, S.; Wooley, K. L.; Pochan, D. J. Block Copolymer Assembly via Kinetic Control. *Science* **2007**, *317* (5838), 647−655.

(9) Gröschel, A. H.; Walther, A.; Löbling, T. I.; Schacher, F. H.; Schmalz, H.; Müller, A. H. E. Guided hierarchical co-assembly of soft patchy nanoparticles. *Nature* **2013**, *503* (7475), 247−251.

(10) Qiu, H.; Hudson, Z. M.; Winnik, M. A.; Manners, I. Multidimensional hierarchical self-assembly of amphiphilic cylindrical block comicelles. *Science* **2015**, *347* (6228), 1329−1332.

(11) Pergushov, D. V.; Müller, A. H. E.; Schacher, F. H. Micellar interpolyelectrolyte complexes. *Chem. Soc. Rev.* **2012**, *41* (21), 6888−6901.

(12) Harada, A.; Kataoka, K. Chain Length Recognition: Core-Shell Supramolecular Assembly from Oppositely Charged Block Copolymers. *Science* **1999**, *283* (5398), 65−67.

(13) Voets, I. K.; de Keizer, A.; de Waard, P.; Frederik, P. M.; Bomans, P. H. H.; Schmalz, H.; Walther, A.; King, S. M.; Leermakers, F. A. M.; Cohen Stuart, M. A. Double-Faced Micelles from Water-Soluble Polymers. *Angew. Chem., Int. Ed.* **2006**, *45* (40), 6673−6676.

(14) Li, M.; Song, W.; Tang, Z.; Lv, S.; Lin, L.; Sun, H.; Li, Q.; Yang, Y.; Hong, H.; Chen, X. Nanoscaled Poly(l-glutamic acid)/Doxorubicin-Amphiphile Complex as pH-responsive Drug Delivery System for Effective Treatment of Nonsmall Cell Lung Cancer. *ACS Appl. Mater. Interfaces* **2013**, *5* (5), 1781−1792.

(15) Dähling, C.; Lotze, G.; Drechsler, M.; Mori, H.; Pergushov, D. V.; Plamper, F. A. Temperature-induced structure switch in thermo-responsive micellar interpolyelectrolyte complexes: toward core-shell-corona and worm-like morphologies. *Soft Matter* **2016**, *12* (23), 5127−5137.

(16) Dähling, C.; Houston, J. E.; Radulescu, A.; Drechsler, M.; Brugnoni, M.; Mori, H.; Pergushov, D. V.; Plamper, F. A. Self-Templated Generation of Triggerable and Restorable Nonequilibrium Micelles. *ACS Macro Lett.* **2018**, *7* (3), 341−346.

(17) Li, J.; Liang, L.; Liang, J.; Wu, W.; Zhou, H.; Guo, J. Constructing Asymmetric Polyion Complex Vesicles via Template Assembling Strategy: Formulation Control and Tunable Permeability. *Nanomaterials* **2017**, *7* (11), 387.

(18) Cai, M.; Ding, Y.; Wang, L.; Huang, L.; Lu, X.; Cai, Y. Synthesis of One-Component Nanostructured Polyion Complexes via Polymer-ization-Induced Electrostatic Self-Assembly. *ACS Macro Lett.* **2018**, *7* (2), 208−212.

(19) Betthausen, E.; Drechsler, M.; Förtsch, M.; Pergushov, D. V.; Schacher, F. H.; Müller, A. H. E. Stimuli-responsive micellar interpolyelectrolyte complexes - control of micelle dynamics via core crosslinking. *Soft Matter* **2012**, *8* (39), 10167−10177.

(20) Xu, W.; Ledin, P. A.; Plamper, F. A.; Synatschke, C. V.; Müller, A. H. E.; Tsukruk, V. V. Multiresponsive Microcapsules Based on Multilayer Assembly of Star Polyelectrolytes. *Macromolecules* **2014**, *47* (22), 7858−7868.

(21) Cui, J.; van Koeverden, M. P.; Müllner, M.; Kempe, K.; Caruso, F. Emerging methods for the fabrication of polymer capsules. *Adv. Colloid Interface Sci.* **2014**, *207* (0), 14−31.

(22) Goto, A.; Yen, H.-C.; Anraku, Y.; Fukushima, S.; Lai, P.-S.; Kato, M.; Kishimura, A.; Kataoka, K. Facile Preparation of Delivery Platform of Water-Soluble Low-Molecular-Weight Drugs Based on Polyion Complex Vesicle (PICsome) Encapsulating Mesoporous Silica Nanoparticle. *ACS Biomater. Sci. Eng.* **2017**, *3* (5), 807−815.

(23) Löbling, T. I.; Haataja, J. S.; Synatschke, C. V.; Schacher, F. H.; Müller, M.; Hanisch, A.; Gröschel, A. H.; Müller, A. H. E. Hidden Structural Features of Multicompartment Micelles Revealed by Cryogenic Transmission Electron Tomography. *ACS Nano* **2014**, *8* (11), 11330−11340.

(24) Synatschke, C. V.; Löbling, T. I.; Förtsch, M.; Hanisch, A.; Schacher, F. H.; Müller, A. H. E. Micellar Interpolyelectrolyte Complexes with a Compartmentalized Shell. *Macromolecules* **2013**, *46* (16), 6466−6474.

(25) Schacher, F. H.; Rudolph, T.; Drechsler, M.; Müller, A. H. E. Core-crosslinked compartmentalized cylinders. *Nanoscale* **2011**, *3* (1), 288−297.

(26) Synatschke, C. V.; Nomoto, T.; Cabral, H.; Förtsch, M.; Toh, K.; Matsumoto, Y.; Miyazaki, K.; Hanisch, A.; Schacher, F. H.; Kishimura, A.; Nishiyama, N.; Müller, A. H. E.; Kataoka, K. Multicompartment Micelles with Adjustable Poly(ethylene glycol) Shell for Efficient in Vivo Photodynamic Therapy. *ACS Nano* **2014**, *8* (2), 1161−1172.

(27) Tsang, B.; Yu, C.; Granick, S. Polymers Zippered-Up by Electric Charge Reveal Themselves. *ACS Nano* **2014**, *8* (11), 11030−11034.

(28) Verduzco, R.; Li, X.; Pesek, S. L.; Stein, G. E. Structure, function, self-assembly, and applications of bottlebrush copolymers. *Chem. Soc. Rev.* **2015**, *44* (8), 2405−2420.

(29) Pelras, T.; Mahon, C. S.; Müllner, M. Synthesis and Applications of Compartmentalised Molecular Polymer Brushes. *Angew. Chem., Int. Ed.* **2018**, *57*, 6982−6994.

(30) Müllner, M. Molecular Polymer Brushes in Nanomedicine. *Macromol. Chem. Phys.* **2016**, *217* (20), 2209−2222.

(31) Müllner, M.; Yuan, J.; Weiss, S.; Walther, A.; Förtsch, M.; Drechsler, M.; Müller, A. H. E. Water-Soluble Organo−Silica Hybrid Nanotubes Templated by Cylindrical Polymer Brushes. *J. Am. Chem. Soc.* **2010**, *132* (46), 16587−16592.

(32) Huang, K.; Rzayev, J. Charge and Size Selective Molecular Transport by Amphiphilic Organic Nanotubes. *J. Am. Chem. Soc.* **2011**, *133* (42), 16726−16729.

(33) Müllner, M.; Lunkenbein, T.; Breu, J.; Caruso, F.; Müller, A. H. E. Template-Directed Synthesis of Silica Nanowires and Nanotubes from Cylindrical Core−Shell Polymer Brushes. *Chem. Mater.* **2012**, *24* (10), 1802−1810.

(34) Ju, Y.; Cui, J.; Sun, H.; Müllner, M.; Dai, Y.; Guo, J.; Bertleff-Zieschang, N.; Suma, T.; Richardson, J. J.; Caruso, F. Engineered Metal-Phenolic Capsules Show Tunable Targeted Delivery to Cancer Cells. *Biomacromolecules* **2016**, *17* (6), 2268−2276.

(35) Radzinski, S. C.; Foster, J. C.; Scannelli, S. J.; Weaver, J. R.; Arrington, K. J.; Matson, J. B. Tapered Bottlebrush Polymers: Cone-Shaped Nanostructures by Sequential Addition of Macromonomers. *ACS Macro Lett.* **2017**, *6* (10), 1175−1179.

(36) Daniel, W. F. M.; Burdyńska, J.; Vatankhah-Varnoosfaderani, M.; Matyjaszewski, K.; Paturej, J.; Rubinstein, M.; Dobrynin, A. V.; Sheiko, S. S. Solvent-free, supersoft and superelastic bottlebrush melts and networks. *Nat. Mater.* **2016**, *15*, 183−189.

(37) Yu-Su, S. Y.; Sheiko, S. S.; Lee, H.-i.; Jakubowski, W.; Nese, A.; Matyjaszewski, K.; Anokhin, D.; Ivanov, D. A. Crystallization of Molecular Brushes with Block Copolymer Side Chains. *Macromolecules* **2009**, *42* (22), 9008−9017.

(38) Malho, J.-M.; Morits, M.; Löbling, T. I.; Nonappa; Majoinen, J.; Schacher, F. H.; Ikkala, O.; Gröschel, A. H. Rod-Like Nanoparticles with Striped and Helical Topography. *ACS Macro Lett.* **2016**, *5* (10), 1185−1190.